DOI: 10.1093/brain/awh007 Advanced Access publication October 21, 2003 *Brain* (2004), **127,** 111–119

Changes in cerebral perfusion precede plaque formation in multiple sclerosis: a longitudinal perfusion MRI study

Jens Wuerfel,[1,3] Judith Bellmann-Strobl,[1] Peter Brunecker,[2] Orhan Aktas,[1] Henry McFarland,[3] Arno Villringer[2] and Frauke Zipp[1]

[1]*Institute of Neuroimmunology, Charité, Berlin,* [2]*Berlin Neuro Imaging Centre, Department of Neurology, Charité, Berlin, Germany and* [3]*Neuroimmunology Branch, NINDS, NIH, Bethesda, MD, USA*

Correspondence to: Frauke Zipp, Professor of Neuroimmunology, Institute of Neuroimmunology, Neuroscience Research Center, NWFZ 2680, Charité University Hospital, 10098 Berlin, Germany
E-mail: frauke.zipp@charite.de

Summary

New MRI techniques such as the analysis of magnetization transfer or diffusion have provided evidence for subtle progressive alterations in tissue integrity prior to focal leakage of the blood–brain barrier (BBB) as part of plaque formation in multiple sclerosis. Since inflammation is capable of modulating the microcirculation, we investigated the hypothesis that changes in the local perfusion might be one of the earliest signs of lesion development. 20 patients with definite relapsing–remitting multiple sclerosis were analysed with regard to cerebral blood volume, cerebral blood flow, mean transit time and apparent diffusion coefficient (ADC), as well as conventional MRI parameters, on monthly follow-up scans. Among 89 gadolinium-enhancing lesions, we selected 18 that developed during the study and met strict inclusion criteria. In these, changes of perfusion parameters were detectable not only prior to the BBB breakdown, but also prior to increases in the ADC. Our data indicate that inflammation is accompanied by altered local perfusion, which can be detected prior to permeability of the BBB.

Keywords: diffusion; longitudinal; MRI; multiple sclerosis; perfusion

Abbreviations: ADC = apparent diffusion coefficient; AIF = arterial input function; BBB = blood–brain barrier; CBF = cerebral blood flow; CBV = cerebral blood volume; EDSS = expanded disability status scale; GdDTPA = gadolinium diethyltriaminepentaacetic acid; MSFC = multiple sclerosis functional composite; MTR = magnetization transfer ratio; MTT = mean transit time; NAWM = normal-appearing white matter; ROI = region of interest; RRMS = relapsing–remitting multiple sclerosis

Introduction

Multiple sclerosis is the most common demyelinating disorder of the CNS. Despite increased insight into the mechanisms of disease (Noseworthy *et al*., 2000; Steinman *et al*., 2002), the precise sequence of events leading to plaque formation, the pathological hallmark of multiple sclerosis, is still not completely understood. The disruption of the blood–brain barrier (BBB) is well recognized as a crucial step in the evolution of the multiple sclerosis lesion (Harris *et al*., 1991; McFarland *et al*., 1992) and is hypothesized to be initiated by autoreactive CD4+ lymphocytes that migrate into the CNS and initiate an inflammatory response (Markovic-Plese and McFarland, 2001). Upregulation of adhesion molecules on capillary endothelial cells, perivascular inflammation, and other factors that facilitate the invasion of leucocytes into the CNS have been studied extensively and are subject to current therapeutic concepts. The gold standard of lesion detection during the course of the disease is the focal enhancement in a T1-weighted MRI after gadolinium diethyltriaminepentaacetic acid (GdDTPA) injection. However, there is more and more evidence indicating changes in the normal-appearing white matter (NAWM) that precede the appearance of new contrast-enhancing lesions. A decrease in magnetization transfer ratio (MTR) is described prior to enhancement, indicating a diminished ability for saturation exchange due to, for example, oedema and inflammation (Filippi *et al*., 1998; Silver *et al*., 1998). Changes in lipid spectra have been noted in magnetic resonance spectroscopy preceding lesions (Wolinsky and Narayana, 2002). Diffusion-weighted imaging

Table 1 *Clinical data at onset of study*

Patient ID	Sex	Age (years)	EDSS	MSFC	Duration of disease (months)
1	F	21	2	–0.644	71
2	F	44	3	0.730	25
3	M	27	1.5	–0.094	7
4	F	42	0	0.307	5
5	F	26	0	–0.448	4
6	F	20	1	0.421	1
7	F	23	1.5	0.195	1
8	F	38	2	0.062	42
9	F	39	0	0.327	17
10	F	31	1	0.494	32
11	F	23	3	–1.424	1
12	F	43	2	–0.123	1
13	F	46	4	–0.926	14
14	F	25	1	0.458	6
15	F	40	3.5	–1.844	187
16	F	30	1	0.180	1
17	F	24	1.5	0.418	44
18	F	34	1.5	0.960	114
19	M	39	2	0.300	33
20	F	26	0	0.652	13

and analysis of the apparent diffusion coefficient (ADC) (Rocca *et al*., 2000; Werring *et al*., 2000) have provided evidence for subtle progressive alterations in tissue integrity several weeks before focal leakage of the BBB and plaque formation. Since an increased ADC reflects elevated levels of random water molecule motion, the observed changes may be due to local metabolic alterations in the inflammatory milieu, such as oedema, prior to tissue damage. However, a major consequence of inflammation, namely local changes in blood flow (Warren, 1994; Moller *et al*., 2002; Perretti and Ahluwalia, 2000) has so far been largely neglected. This prompted us to investigate changes in the perfusion of plaques and potential areas of plaque formation in combination with changes in the ADC in a longitudinal study. The overall aim was to further understand the process of lesion formation *in vivo*, which in patients can only be followed by imaging methods.

Material and methods

Patients

We studied 20 patients (18 female) meeting the newly introduced criteria for relapsing–remitting multiple sclerosis (RRMS) (McDonald *et al*., 2001) over a mean period of 11.4 months (range 5–23) with biweekly/monthly MRI examinations. Patients were enrolled at the Institute of Neuroimmunology, Outpatient Clinic, Department of Neurology, Charité University Hospital, Berlin, Germany and followed up regularly for clinical parameters, i.e. evaluation of expanded disability status scale (EDSS) and multiple sclerosis functional composite (MSFC) scores (Kurtzke, 1983; Fischer *et al*., 1999). Signed, informed consent was obtained from all participating subjects. Patients presented with mean disease duration of 30.9 months (range 1–187) and an EDSS score of 1.6 (range 0–4) (Table 1). During the study, three patients were started on disease-modifying therapy (two patients with interferon-β1a, one patient with glatiramer acetate).

MRI

MRI measurements were performed on a scanner operating at 1.5 T (Siemens Vision; Siemens Medical Systems, Erlangen, Germany). The MRI protocol consisted of T2-weighted imaging, T1-weighted imaging before and 5 min after GdDPTA injection (Magnevist®; Schering AG, Berlin, Germany), diffusion-weighted images and T2*-weighted dynamic susceptibility contrast perfusion measurement. For T2-weighted imaging a multi-echo turbo-spin-echo sequence was used [repetition time (TR) 4060 ms, echo time (TE) 15/75/135 ms, matrix 256 × 256, acquisition time 345 s, field of view (FOV) 256 mm, slice thickness 5 mm, no gap, 28 slices], and for T1-weighted imaging a spin-echo sequence (TR 840 ms, TE 14 ms, matrix 256 × 256, acquisition time 164 s, FOV 256 mm, slice thickness 5 mm, no gap, 28 slices) was employed. Intravenous injection of 0.20 mmol/kg body weight GdDPTA was performed with a MRI compatible power injector (Spectris; MedRad, Pittsburgh, PA, USA) at an injection rate of 4 ml/s (5 s duration) followed by 20 ml saline. MRI data acquisition started at the beginning of the contrast agent injection with a temporal resolution of 1 s and was continued for 60 s.

Perfusion measurements were performed using a T2*-weighted echo-planar sequence (TR 800 ms, TE 54 ms, matrix 128 × 128, acquisition time 60 s, FOV 256 mm, slice thickness 5 mm, no gap) (Doege *et al*., 2001). In order to measure the bolus transit through the tissue at a reasonable temporal resolution, we selected only eight slices for the perfusion measurement. Spin-echo diffusion echo-

planar imaging (TR 4000 ms, TE 118 ms, matrix 128 × 128, acquisition time 208 s, FOV 256 mm, slice thickness 5 mm, no gap) was performed using three different b values (0, 500, 1000 s/mm^2). Diffusion gradients were applied in three orthogonal directions. Twenty-eight axial slices were positioned in anterior commissure–posterior commissure orientation. Slices of T1-, T2- and perfusion-weighted images had the same orientation.

Image analysis

Bulk white matter lesion load of T2-weighted scans and number and volume of hypo- and hyperintense lesions on T1-weighted scans were routinely measured using MedX© v. 3.42 software package (Sensor Systems Inc., Sterling, VA, USA). Diffusion-weighted images were preprocessed immediately after acquisition as part of the sequence used. The ADC was calculated separately for each direction. Preprocessed data were transferred to a LINUX workstation for further analysis. For the analysis of the perfusion-weighted images, selected voxels of the baseline scan exhibiting high and early contrast influx were used for the measurement of the arterial input function (AIF). Identical voxels were used in all registered scans for subsequent AIF measurement. Perfusion-weighted images were first corrected for BBB leakage artefacts, using a paradigm described by Haselhorst *et al*. (2000). An internal threshold enabled us to reliably correct only voxels that were affected by the leakage. Corrected data were then processed with MedX perfusion data analysis package. Pixel based calculations, with subsequent generation of relative cerebral blood volume (CBV), cerebral blood flow (CBF) and mean transit time (MTT), were performed as described by Ostergaard *et al*. (2000). We used relative perfusion values, since the determination of absolute perfusion values is still controversial based on magnetic resonance bolus-tracking techniques currently in use.

In order to exactly compare different time points and magnetic resonance sequences, T1-, T2-, diffusion-weighted and T2* images were spatially co-registered using an automated six-parameter rigid body image registration with trilinear interpolation [FMRIB's Linear Image Registration Tool (FLIRT); FMRIB Analysis Group, University of Oxford, Oxford, UK] (Jenkinson and Smith, 2001). Registered T2* images were used for subsequent calculation of CBV, CBF and MTT maps. An example of the alignment of T1- and T2-weighted images, ADC and CBV-maps is shown in Fig. 1. Regions of interest (ROIs) were drawn on lesions visible on T1-enhanced scans, copied to the other sets, respectively, and followed longitudinally. These ROIs were flipped to the contralateral hemisphere to create an unbiased, corresponding localization in NAWM without any GdDTPA enhancement throughout the longitudinal study and expressed as ratios (lesion/contralateral NAWM).

For the analysis of the perfusion-weighted images in regions of lesion formation, we applied the following inclusion criteria. To avoid partial volume effects, especially due to the registration process, we excluded all lesions that were adjacent to the CSF/ventricles. All lesions close to the grey–white matter boundary were also excluded, due to the fact that perfusion of grey matter and white matter differ significantly. Only lesions with a diameter of at least 7 mm were included, to assure sufficient reliability in a longitudinal study.

Three lesions developed a ring enhancement on T1-weighted scans. In these lesions we measured the perfusion of the contrast-enhancing ring and the hypointense interior seperately.

Statistical analysis

The scan at which GdDTPA enhancement was first noted defined the reference time point (time = 0) for the longitudinal measurements. To evaluate the evolution of lesions prior to appearance on GdDTPA-enhanced T1-weighted images, Wilcoxon signed rank tests were performed to compare CBV, CBF, MTT and ADC ratios (lesion/contralateral NAWM) at different intervals.

Results

Clinical data and selection of lesions

Among 20 patients with RRMS (Table 1), 15 untreated patients developed gadolinium-enhancing lesions during the course of the study. In total, 89 contrast-enhancing lesions were detected; out of these 39 were detectable on the slices covered by the perfusion. A total of 18 lesions in seven patients met our inclusion criteria, among which three had ring enhancement (Table 2). We statistically analysed the data referring to nine lesions for which at least two baseline scans were available exceeding 6 weeks prior to GdDTPA enhancement.

During the periods of lesion formation analysed, no significant changes of disability measured by EDSS and MSFC were detected (data not shown).

Establishment of a leakage correction algorithm

A conspicuous artefact observed in perfusion maps of gadolinium-enhancing lesions, which is due to the leakage of some contrast agent through the BBB, can be overcome by fitting a model function for the plasma concentration to the measured data, as described by Haselhorst *et al*. (2000). We calculated perfusion maps with data to which we had applied a leakage correction algorithm prior to calculation and compared these data with uncorrected images (Fig. 2). The concentration versus time curves obtained from acutely gadolinium-enhancing plaques show a dramatic signal overshoot and a subsequent drop below the baseline in the non-corrected image (Fig. 2A), due to a significant reduction in T1 relaxation time that is caused by the leakage of some contrast agent into the interstitial space. This leads to a signal increase, owing to the short repetition time of our sequence, but also to a significant underestimation of the integral taken as a measure of CBV. Figure 2B shows the same concentration versus time curve with prior application of the leakage correction algorithm. The integral of the corrected curve is up to 55% higher than the pre-correction value. For non-enhancing white matter areas, no significant difference was detected between any corrected and uncorrected perfusion maps (Fig. 2C and D).

Perfusion and ADC measurements before and after GdDTPA enhancement

In the course of the selected lesions revealing gadolinium enhancement at time = 0, we were specifically interested in

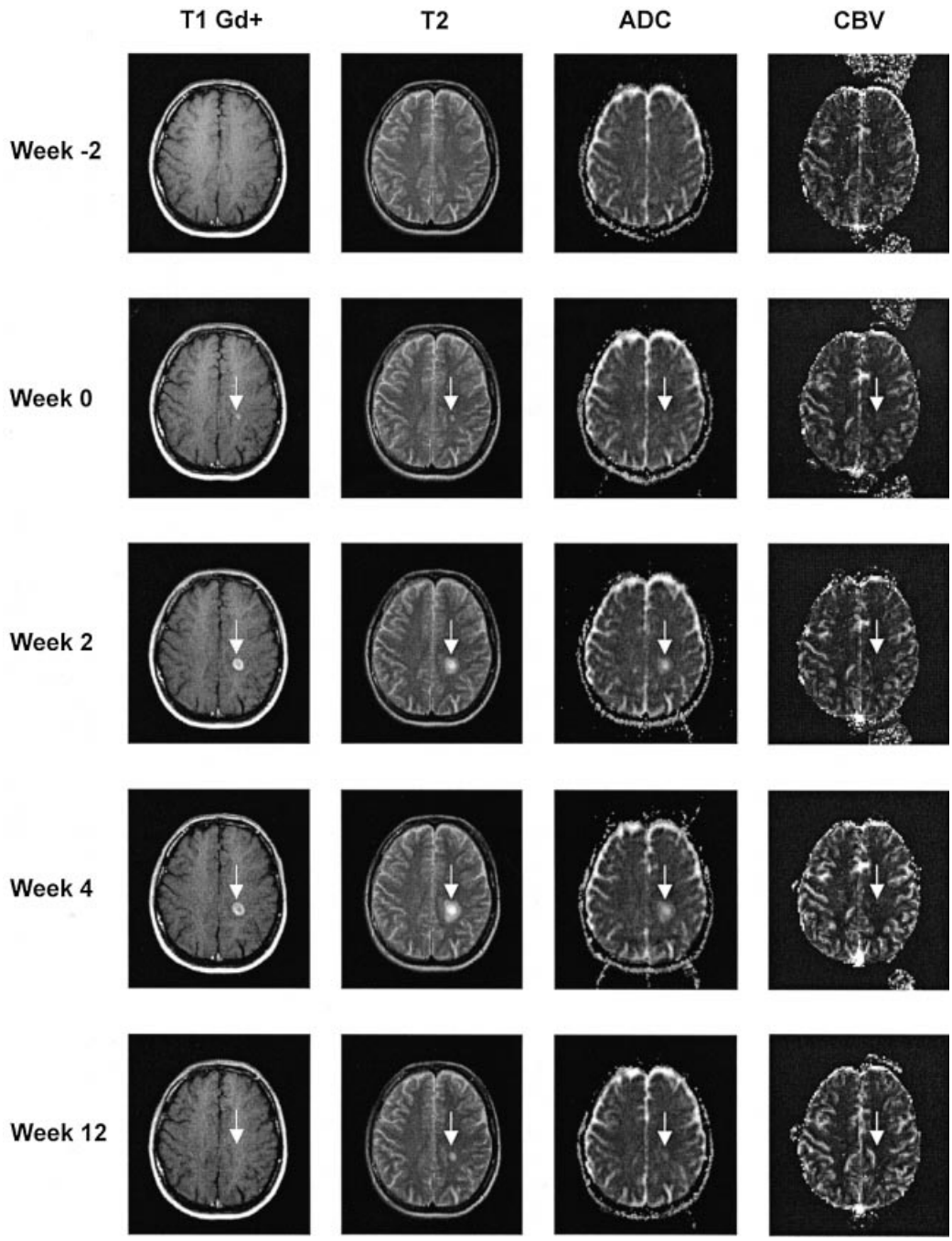

Fig. 1 Co-registration of T1- and T2-weighted images, and ADC and CBV maps. The development of a lesion is presented in a series of GdDTPA enhanced T1-weighted scans and in co-registered T2-weighted images, and ADC and CBV maps at 2 weeks prior to enhancement, time of the first enhancement, and 2, 4 and 12 weeks thereafter.

investigating CBV, CBF, MTT and ADC. A representative example of these measurements of lesion development is given in Fig. 3.

A rapid increase in ADC of lesion area compared with the corresponding contralateral NAWM was detected in all lesions studied at the time of initial enhancement. While this elevation was statistically significant, a smaller increase in ADC up to 3 weeks (range 2–4) prior to enhancement was seen only in three series of lesion development and was not statistically significant ($P = 0.173$; Wilcoxon signed rank; Table 3). The ADC remained slightly above baseline values in all lesions studied after the BBB leakage stopped until the end of the study period.

The perfusion measurements analysed in those lesions showed alterations for CBV and CBF, while there were no statistically relevant changes in MTT. In each lesion studied

Table 2 *Observed contrast-enhancing lesions*

Patient ID	Total number of lesions	Number of lesions included
1	1	0
2	6	0
3	1	0
4	0	0
5	0	0
6	8	5
7	10	0
8	1	0
9	9	3
10	0	0
11	0	0
12	5	2
13	1	1
14	0	0
15	22	0
16	3	3
17	19	2
18	2	2
19	0	0
20	0	0
Total	89	18

prior to enhancement, we found a significant increase of CBV and CBF, not only at the time of initial GdDTPA enhancement in comparison with the baseline (CBV $P = 0.008$; CBF $P = 0.015$; Wilcoxon signed rank), but also in pre-lesion ROI as early as 3 weeks (range 2–4) prior to BBB leakage (CBV $P = 0.008$; CBF $P = 0.008$; Wilcoxon signed rank; Table 3).

In fact, 3 weeks before GdDTPA enhancement CBV and CBF showed an increase from baseline of 18 and 17.9%, respectively. Comparing 3 weeks prior to enhancement with the time of BBB breakdown, no significant differences in CBV and CBF were observed. These results clearly emphasize early blood flow changes during the development of these multiple sclerosis lesions. CBV and CBF remained above baseline values for several weeks after the BBB breakdown had ceased, as shown in an overlay of all longitudinal data for the 18 lesions that fulfilled the inclusion criteria for the analysis of local perfusion changes (Fig. 4).

Plaques with ring enhancement

In three lesions that developed ring enhancement after contrast agent injection, patterns of CBV and CBF changes comparable to non-ring-enhancing lesions were seen only in the 'ring tissue'. In line with our main finding of increased perfusion in the area of BBB breakdown, presumably due to

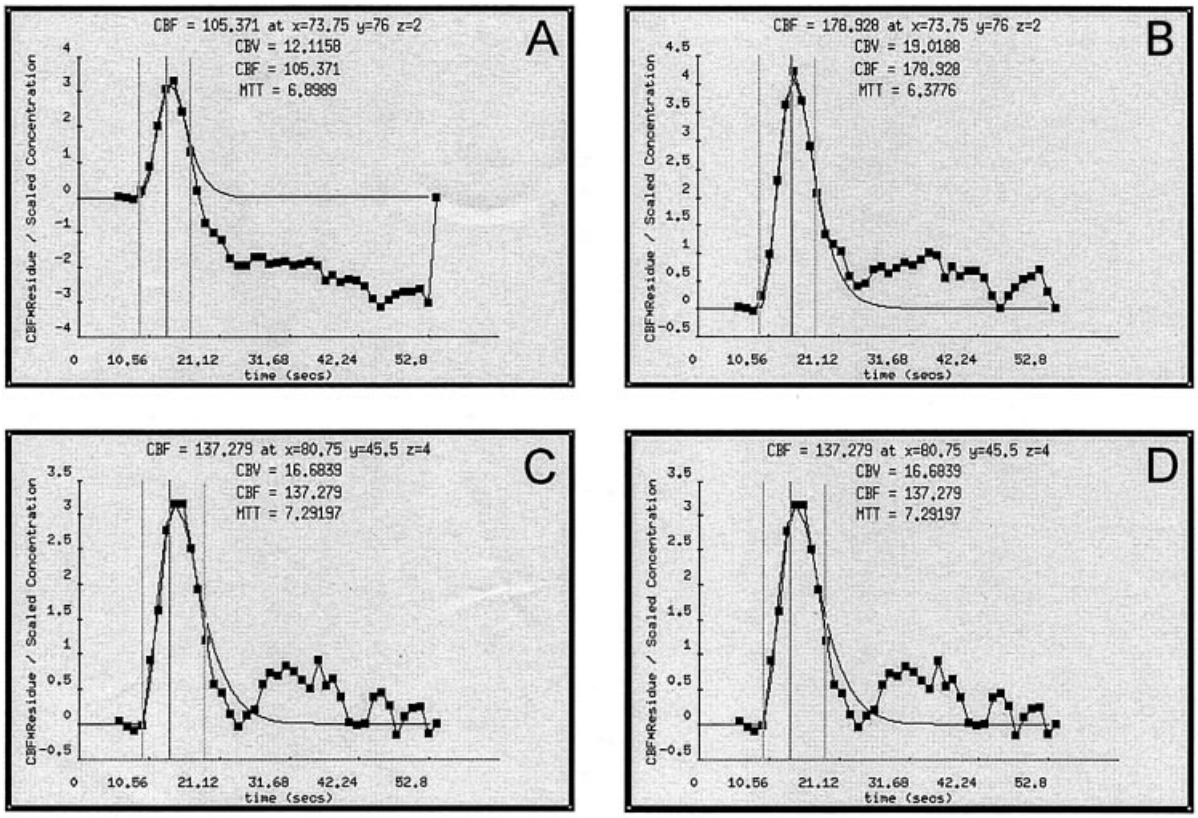

Fig. 2 Impact of a leakage correction paradigm on signal intensity over time. Signal versus time curves were measured in a contrast-enhancing lesion without (**A**) and with (**B**) application of a leakage correction paradigm described by Haselhorst *et al*. (2000). The non-enhancing NAWM of the contralateral side does not show any significant changes before (**C**) and after (**D**) correction.

inflammation, CBV and CBF exhibited higher levels in the region of the ring enhancement than the centre of these lesions, which appeared hypointense on T1-weighted images. Thus, only the region of the enhanced ring was included in our overall perfusivity determination of vascular changes (see Table 3). Table 4 presents CBV, CBF and MTT values separately for the region of the gadolinium-enhanced ring and the non-enhancing inner part of the lesion, as defined by the T1-weighted image.

Development of T1-hypointensity

In two lesions that became hypointense on T1-enhanced scans ('black holes'), several weeks after GdDTPA enhancement, CBV and CBF eventually dropped below baseline values (data not shown). This finding is in line with a previous report of reduced CBV in T1-hypointense lesions in a cross-sectional study (Haselhorst *et al*., 2000), and may well be the result of severe tissue destruction and gliosis, as suggested by magnetization transfer and spectroscopy studies (van Waesberghe *et al*., 1999; Li *et al*., 2003).

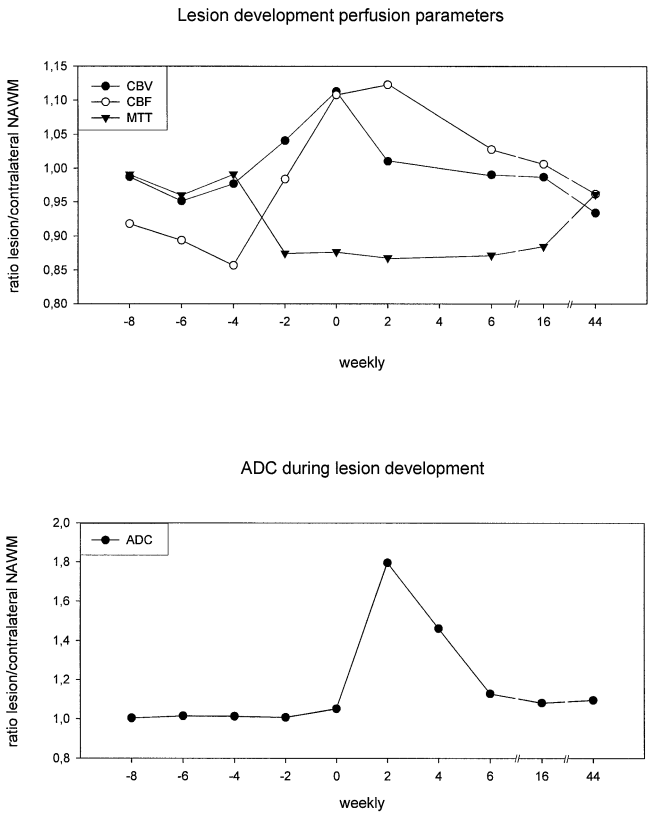

Fig. 3 A representative example of time courses for perfusion and diffusion parameters during plaque formation. CBV, CBF, MTT and ADC are shown. Time point 0 was defined as first GdDTPA enhancement visible on T1-weighted images.

Discussion

Perfusion-weighted imaging has so far not become an element of the MRI techniques relevant for multiple sclerosis (Miller *et al*., 1998). This might be due to the fact that perfusion studies are technically challenging and at present still of lower resolution than other MRI techniques. To our knowledge, the present MRI study on perfusion measurements of multiple sclerosis lesion development is the first longitudinal investigation of its kind, and opens up new insights into the mechanisms of neuroinflammatory plaque formation. Our findings confirm the hypothesis that lesion formation actually begins several weeks before becoming evident on GdDTPA enhanced scans. In fact, a steep regional increase of CBV and CBF compared with the contralateral side could be detected up to 3 weeks prior to the breakdown of the BBB and subsequent contrast enhancement, indicating a dominant role of the vasculature preceding the inflammation of white matter tissue. The proximity of evolving plaques to venules is a well described feature in multiple sclerosis (Lucchinetti *et al*., 1998). In several models of neuroinflammation, various effects on the circulation by inflammation- and cytotoxicity-mediating substances were reported. This might be due to different steps of the inflammatory processes being targeted by the different models. An increased permeability in the region of the BBB and higher CBVs were observed after intrathekal application of interleukin-1β (Blamire *et al*., 2000). The reduction of the CBV observed in response to direct intrastriatal injection of tumour necrosis factor-α (Sibson *et al*., 2002) might reflect a rather late stage of inflammation. In fact, other substances presumably originating during brain inflammation in multiple sclerosis, such as nitric oxide and substance P, are classical vasodilators (Kostyk *et al*., 1989; Hartung and Kieseier, 1996).

Table 3 *CBV, CBF and ADC ratios during lesion formation*

Weeks before enhancement	Mean CBV ratio (SD), $n = 9$	*P* value	Mean CBF ratio (SD), $n = 9$	*P* value	Mean ADC ratio (SD), $n = 9$	*P* value
Baseline (>6)	1.0288 (0.182)		1.0601 (0.226)		1.0626 (0.107)	
3 (±1)	1.2154 (0.245)	0.008	1.2506 (0.259)	0.008	1.0489 (0.093)	0.173
0	1.2603 (0.265)	0.008	1.3144 (0.268)	0.015	1.2845 (0.295)	0.011

Mean values and SDs are shown. *P*-values are given for changes of CBV, CBF and ADC in comparison with the baseline (Wilcoxon signed rank test).

In the present study, an increase of perfusion was already found prior to the elevation of the diffusivity (ADC), indicating local blood flow changes early during the plaque formation process. Whereas changes in the perfusion measurements represent functional characteristics of a certain condition of the vasculature and its vicinity (Barbier *et al*., 2001), alterations in the apparent water diffusion rate reflect pathological changes in the brain tissue due to the diffusion characteristics of the intra- and extracellular water compartments (Gass *et al*., 2001). Accordingly, several stroke studies have shown a reduction of the ADC in areas of ischaemia and cytotoxic oedema (Moseley *et al*., 1990; Mintorovitch *et al*., 1994). An inverse relationship between diffusion and perfusion was revealed in some epilepsy studies, where a close correlation of reduced diffusion and signs of regional hyperperfusion after prolonged ictal activity on magnetic resonance angiography could be demonstrated (Wieshmann *et al*., 1997; Lansberg *et al*., 1999). A similar phenomenon has been described in functional MRI experiments. Here, an activation of certain areas after stimulation caused an increase in regional blood flow as measured by blood oxygen level-dependent contrast (Bandettini *et al*., 1992) or contrast agent perfusion techniques (Belliveau *et al*., 1991), but interestingly it also lead to a transient decrease of the ADC in the same area (Darquie *et al*., 2001). In multiple sclerosis, vasogenic oedema and an increase of extracellular space in combination with myelin breakdown and tissue structure disruption were reported to result in increased ADC values in both, NAWM (Rocca *et al*., 2000; Werring *et al*., 2000; Cercignani *et al*., 2001; Caramia *et al*., 2002), and acute and chronic lesions (Tievsky *et al*., 1999; Filippi *et al*., 2000). Interestingly, a prominent perfusion increase was found prior to a significant increase in ADC in the present study. The peak of the CBV was followed by a gradual decline over 20 weeks, before it decreased more rapidly, and, in case of development of T1-hypointensity ('black hole'), remained below baseline. The initial elevation can presumably be explained by inflammation-related vasodilation in the acute stage, whereas the decreased perfusion in later stages of the lesion might be due to the development of a (hypometabolic) gliotic scar, which is indicated by reduced *N*-acetyl-aspartate (NAA)/creatine ratios in magnetic resonance spectroscopy in T1-hypointense lesions (van Walderveen *et al*., 1998; Li *et al*., 2003).

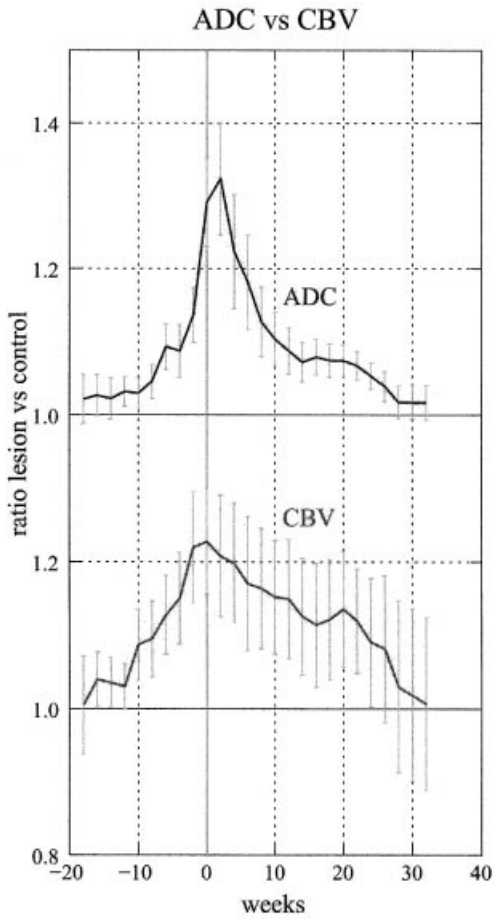

Fig. 4 Mean ADC and CBV in all selected lesions (n = 18). Evolution of ADC and CBV ratios in 18 lesions. Time point 0 was defined as first GdDTPA enhancement visible on T1-weighted images. Mean values (curve points) and SDs (vertical lines) are given for the number of corresponding intervals. The number of observations was lower at early and late time points compared with the number of observations at time point 0 (minimum number ⩾5).

Three lesions developed a ring-like appearance on GdDTPA-enhanced scans. In such lesions the MTR, a measure of tissue damage (van Waesberghe *et al*., 1999), was found to be lowest inside the T1-hypointense centre (Hiehle *et al*., 1995). These reports support our finding of reduced CBV and CBF inside those plaques. One may speculate that the reduced blood supply in such lesions accounts for a higher probability of permanent tissue destruction, which might be an explanation for the

Table 4 *Perfusion values (SD) of ring-enhancing lesions*

Lesion	CBV ring	CBV inside	CBF ring	CBF inside	MTT ring	MTT inside
1	15.48 (8.6)	10.26 (4.73)	158 (96.26)	93.84 (44.9)	6.04 (1.37)	6.7 (1.45)
2	9.25 (4.1)	8.7 (3.83)	88.38 (43.9)	70.25 (27.53)	6.17 (1.67)	7.4 (1.2)
3	21.17 (5.74)	16.18 (1.21)	211.41 (58.5)	148.53 (20.4)	6.04 (0.44)	6.59 (0.64)

CBV and CBF are higher, MTT is faster in the area of the GdDTPA-enhanced ring compared with the inside region that remains hypointense on T1-weighted images in three ring-enhancing lesions.

observation that ring-enhancing lesions account for a more destructive disease course (Morgen *et al*., 2001).

Taken together, our data on cerebral blood perfusion measurements during lesion formation in multiple sclerosis patients with relapsing–remitting disease course indicate that elevation of perfusion is an early event in the development of a plaque. Improving the resolution of this technique might not only give new insight into the pathomechanisms in multiple sclerosis, but also lead to a more sensitive measurement of disease activity and treatment effects (Miller, 1996; McFarland *et al*., 2002).

Acknowledgements

We wish to thank Reta Haselhorst for providing a leakage correction paradigm, Andrea Rebmann and Jeff Quinlivan for introduction to the MedX perfusion module, Bianca Müller for assistance with scanning procedures, and Celia Forbes for carefully editing the manuscript for english. This work was supported by grants from the Bundesministerium für Bildung und Forschung (BMBF) and the Gemeinnützige Hertie Stiftung. J.W. was supported by the Boehringer Ingelheim Fonds (BIF).

References

Bandettini PA, Wong EC, Hinks RS, Tikofsky RS, Hyde JS. Time course EPI of human brain function during task activation. Magn Reson Med 1992; 25: 390–7.

Barbier EL, Lamalle L, Decorps M. Methodology of brain perfusion imaging. J Magn Reson Imaging 2001; 13: 496–520.

Belliveau JW, Kennedy DN Jr, McKinstry RC, Buchbinder BR, Weisskoff RM, Cohen MS, et al. Functional mapping of the human visual cortex by magnetic resonance imaging. Science 1991; 254: 716–9.

Blamire AM, Anthony DC, Rajagopalan B, Sibson NR, Perry VH, Styles P. Interleukin-1beta-induced changes in blood–brain barrier permeability, apparent diffusion coefficient, and cerebral blood volume in the rat brain: a magnetic resonance study. J Neurosci 2000; 20: 8153–9.

Caramia F, Pantano P, Di Legge S, Piatella MC, Lenzi D, Paolillo A, et al. A longitudinal study of MR diffusion changes in normal appearing white matter of patients with early multiple sclerosis. Magn Reson Imaging 2002; 20: 383–8.

Cercignani M, Iannucci G, Rocca MA, Comi G, Horsfield MA, Filippi M. Pathologic damage in MS assessed by diffusion-weighted and magnetization transfer MRI. Neurology 2000; 54: 1139–44.

Cercignani M, Inglese M, Pagani E, Comi G, Filippi M. Mean diffusivity and fractional anisotropy histograms of patients with multiple sclerosis. AJNR Am J Neuroradiol 2001; 22: 952–8.

Darquie A, Poline JB, Poupon C, Saint-Jalmes H, Le Bihan D. Transient decrease in water diffusion observed in human occipital cortex during visual stimulation. Proc Natl Acad Sci USA 2001; 98: 9391–5.

Doege CA, Tavakolian R, Kerskens CM, Romero BI, Lehmann R, Einhaupl KM, et al. Perfusion and diffusion magnetic resonance imaging in human cerebral venous thrombosis. Neurology 2001; 248: 564–71.

Filippi M, Rocca MA, Martino G, Horsfield MA, Comi G. Magnetization transfer changes in the normal appearing white matter precede the appearance of enhancing lesions in patients with multiple sclerosis. Ann Neurol 1998; 43: 809–14.

Filippi M, Iannucci G, Cercignani M, Rocca MA, Pratesi A, Comi G. A quantitative study of water diffusion in multiple sclerosis lesions and normal-appearing white matter using echo-planar imaging. Arch Neurol 2000; 57: 1017–21.

Fischer JS, Rudick RA, Cutter GR, Reingold SC. The Multiple Sclerosis Functional Composite Measure (MSFC): an integrated approach to MS clinical outcome assessment. National MS Society Clinical Outcomes Assessment Task Force. Mult Scler 1999; 5: 244–50.

Gass A, Niendorf T, Hirsch JG. Acute and chronic changes of the apparent diffusion coefficient in neurological disorders—biophysical mechanisms and possible underlying histopathology. J Neurol Sci 2001; 186 Suppl 1: S15–23.

Harris JO, Frank JA, Patronas N, McFarlin DE, McFarland HF. Serial gadolinium-enhanced magnetic resonance imaging scans in patients with early, relapsing-remitting multiple sclerosis: implications for clinical trials and natural history. Ann Neurol 1991; 29: 548–55.

Hartung HP, Kieseier BC. Targets for the therapeutic action of interferon-beta in multiple sclerosis. Ann Neurol 1996; 40: 825–6.

Haselhorst R, Kappos L, Bilecen D, Scheffler K, Mori D, Radu EW, et al. Dynamic susceptibility contrast MR imaging of plaque development in multiple sclerosis: application of an extended blood–brain barrier leakage correction. J Magn Reson Imaging 2000; 11: 495–505.

Hiehle JF Jr, Grossman RI, Ramer KN, Gonzalez-Scarano F, Cohen JA. Magnetization transfer effects in MR-detected multiple sclerosis lesions: comparison with gadolinium-enhanced spin-echo images and nonenhanced T1-weighted images. AJNR Am J Neuroradiol 1995; 16: 69–77.

Jenkinson M, Smith S. A global optimisation method for robust affine registration of brain images. Med Image Anal 2001; 5: 143–56.

Kagstrom E, Smith ML, Siesjo BK. Local cerebral blood flow in the recovery period following complete cerebral ischemia in the rat. J Cereb Blood Flow Metab 1983; 3: 170–82.

Kostyk SK, Kowall NW, Hauser SL. Substance P immunoreactive astrocytes are present in multiple sclerosis plaques. Brain Res 1989; 504: 284–8.

Kurtzke JF. Rating neurologic impairment in multiple sclerosis: an expanded disability status scale (EDSS). Neurology 1983; 33: 1444–52.

Lansberg MG, O'Brien MW, Norbash AM, Moseley ME, Morrell M, Albers GW. MRI abnormalities associated with partial status epilepticus. Neurology 1999; 52: 1021–7.

Li BS, Regal J, Soher BJ, Mannon LJ, Grossman RI, Gonen O. Brain metabolite profiles of T1-hypointense lesions in relapsing–remitting multiple sclerosis. AJNR Am J Neuroradiol 2003; 24: 68–74.

Lucchinetti CF, Brueck W, Rodriguez M, Lassmann H. Multiple sclerosis: lessons from neuropathology. Semin Neurol 1998; 18: 337–49.

Markovic-Plese S, McFarland HF. Immunopathogenesis of the multiple sclerosis lesion. Curr Neurol Neurosci Rep 2001; 1: 257–62.

McDonald WI, Compston A, Edan G, Goodkin D, Hartung HP, Lublin FD, et al. Recommended diagnostic criteria for multiple sclerosis: guidelines from the International Panel on the diagnosis of multiple sclerosis. Ann Neurol 2001; 50: 121–7.

McFarland HF, Frank JA, Albert PS, Smith ME, Martin R, Harris JO, et al. Using gadolinium-enhanced magnetic resonance imaging lesions to monitor disease activity in multiple sclerosis. Ann Neurol 1992; 32: 758–66.

McFarland HF, Barkhof F, Antel J, Miller DH. The role of MRI as a surrogate outcome measure in multiple sclerosis. Mult Scler 2002; 8: 40–51.

Miller DH. The use of MRI in monitoring the treatment of multiple sclerosis. Ital J Neurol Sci 1996; 17: 383–4.

Miller DH, Grossman RI, Reingold SC, McFarland HF. The role of magnetic resonance techniques in understanding and managing multiple sclerosis. Brain 1998; 121: 3–24.

Mintorovitch J, Yang GY, Shimizu H, Kucharczyk J, Chan PH, Weinstein PR. Diffusion-weighted magnetic resonance imaging of acute focal cerebral ischemia: comparison of signal intensity with changes in brain water and Na+,K(+)-ATPase activity. J Cereb Blood Flow Metab 1994; 14: 332–6.

Moller K, Strauss GI, Qvist J, Fonsmark L, Knudsen GM, Larsen FS, et al. Cerebral blood flow and oxidative metabolism during human endotoxemia. J Cereb Blood Flow Metab 2002; 22: 1262–70.

Morgen K, Jeffries NO, Stone R, Martin R, Richert ND, Frank JA, et al.

Ring-enchancement in multiple sclerosis: marker of disease severity. Mult Scler 2001; 7: 167–71.

Moseley ME, Cohen Y, Mintorovitch J, Chileuitt L, Shimizu H, Kucharczyk J, et al. Early detection of regional cerebral ischemia in cats: comparison of diffusion- and T2-weighted MRI and spectroscopy. Magn Reson Med 1990; 14: 330–46.

Noseworthy JH, Lucchinetti C, Rodriguez M, Weinshenker BG. Multiple sclerosis. New Engl J Med 2000; 343: 938–52.

Ostergaard L, Sorensen AG, Chesler DA, Weisskoff RM, Koroshetz WJ, Wu O, et al. Combined diffusion-weighted and perfusion-weighted flow heterogeneity magnetic resonance imaging in acute stroke. Stroke 2000; 31: 1097–103.

Perretti M, Ahluwalia A. The microcirculation and inflammation: site of action for glucocorticoids. Microcirculation 2000; 7: 147–61.

Rocca MA, Cercignani M, Iannucci G, Comi G, Filippi M. Weekly diffusion-weighted imaging of normal-appearing white matter in MS. Neurology 2000; 55: 882–4.

Sibson NR, Blamire AM, Perry VH, Gauldie J, Styles P, Anthony DC. TNF-alpha reduces cerebral blood volume and disrupts tissue homeostasis via an endothelin- and TNFR2-dependent pathway. Brain 2002; 125: 2446–59.

Silver NC, Lai M, Symms MR, Barker GJ, McDonald WI, Miller DH. Serial magnetization transfer imaging to characterize the early evolution of new MS lesions. Neurology 1998; 51: 758–64.

Steinman L, Martin R, Bernard C, Conlon P, Oksenberg JR. Multiple sclerosis: deeper understanding of its pathogenesis reveals new targets for therapy. Annu Rev Neurosci 2002; 25: 491–505.

Tievsky AL, Ptak T, Farkas J. Investigation of apparent diffusion coefficient and diffusion tensor anisotrophy in acute and chronic multiple sclerosis lesions. AJNR Am J Neuroradiol 1999; 20: 1491–9.

van Waesberghe JH, Kamphorst W, De Groot CJ, van Walderveen MA, Castelijns JA, Ravid R, et al. Axonal loss in multiple sclerosis lesions: magnetic resonance imaging insights into substrates of disability. Ann Neurol 1999; 46: 747–54.

van Walderveen MA, Kamphorst W, Scheltens P, van Waesberghe JH, Ravid R, Valk J, et al. Histopathologic correlate of hypointense lesions on T1-weighted spin-echo MRI in multiple sclerosis. Neurology 1998; 50: 1282–8.

Warren JB. Nitric oxide and human skin blood flow responses to acetylcholine and ultraviolet light. FASEB J 1994; 8: 247–51.

Werring DJ, Brassat D, Droogan AG, Clark CA, Symms MR, Barker GJ, et al. The pathogenesis of lesions and normal-appearing white matter changes in multiple sclerosis: a serial diffusion MRI study. Brain 2000; 123: 1667–76.

Wieshmann UC, Symms MR, Shorvon SD. Diffusion changes in status epilepticus. Lancet 1997; 350: 493–4.

Wolinsky JS, Narayana PA. Magnetic resonance spectroscopy in multiple sclerosis: window into the diseased brain. Curr Opin Neurol 2002; 15: 247–51.

Received June 2, 2003. Revised August 5, 2003
Accepted August 7, 2003